



Personalized medicine

Holmium–lipiodol–alginate microspheres for fluoroscopy-guided embolotherapy and multimodality imaging



Chris Oerlemans^{a,*}, Peter R. Seevinck^a, Maarten L. Smits^a, Wim E. Hennink^b,
Chris J.G. Bakker^a, Maurice A.A.J. van den Bosch^a, J. Frank W. Nijsen^a

^a Department of Radiology, University Medical Center Utrecht, Utrecht, The Netherlands

^b Department of Pharmaceutics, Utrecht University, Utrecht, The Netherlands

ARTICLE INFO

Article history:

Received 29 May 2014

Received in revised form 30 October 2014

Accepted 4 November 2014

Available online 6 November 2014

Keywords:

Embolization

Microspheres

Lipiodol

Magnetic resonance imaging (MRI)

Computed tomography (CT)

X-ray

ABSTRACT

Embolotherapy is a minimally invasive transcatheter technique aiming at reduction or complete obstruction of the blood flow by infusion of micro-sized particles in order to induce tumor regression. A major drawback of the current commercially available and clinically used microspheres is that they cannot be detected in vivo with medical imaging techniques, impeding intra- and post-procedural feedback. It can be expected that real-time monitoring of microsphere infusion and post-procedural imaging will result in better predictability and higher efficacy of the treatment. In this study, a novel microsphere formulation has been developed that can be visualized with fluoroscopy, X-ray computed tomography (CT) and magnetic resonance imaging (MRI). The microspheres were prepared with the JetCutter technique and consist of alginate (matrix-forming polymer), holmium (cross-linking and MRI contrast agent), lipiodol (radiopaque contrast agent) and Pluronic F-68 (surfactant). The mean size (\pm SEM) of the hydrated holmium–lipiodol–alginate microspheres (Ho–lip–ams) was $570 \pm 12 \mu\text{m}$ with a holmium content of $0.38 \pm 0.01\%$ (w/w). Stability studies showed that the microspheres remained intact during incubation for two weeks in fetal calf serum (FCS) at 37°C . The inclusion of lipiodol in the microspheres rendered excellent visualization capabilities for fluoroscopy and CT, whereas the holmium ions, which keep the alginate network together, also allow MR imaging. In this study it was shown that single sphere detection was possible by fluoroscopy, CT and MRI. The Ho–lip–ams were visualized in real-time, during infusion in a porcine kidney using fluoroscopy, and post-procedural, the deposition of the microspheres was examined with fluoroscopy, (cone beam rotational) CT and MRI. The different imaging modalities showed similar deposition patterns of the microspheres within the organ. The combination of intra-procedural visualization, multimodality imaging for patient follow-up and the possibility of quantification offers a new and promising method for more safe, efficient and successful embolization treatment.

© 2014 Elsevier B.V. All rights reserved.

1. Introduction

Embolotherapy, i.e., intra-arterial injection of embolic agents, has gained an important position in the treatment of a wide variety of conditions affecting different organs of the human body, such as uterine fibroids, arteriovenous malformations (AVM), as well as kidney and liver tumors. Embolotherapy is a minimally invasive transcatheter technique aiming at reduction or complete obstruction of the blood flow by infusion of micro-sized particles of a predefined size in order to induce tumor regression. Several embolotherapy agents are commercially available and clinically

used, ranging from heterodisperse, irregularly shaped, polyvinyl alcohol (PVA) particles (Derdeyn et al., 1995), to spherically shaped and uniformly sized microspheres such as Embosphere (Merit Medical, South Jordan, Utah, USA) (Merit Medical, 2014, <http://www.merit.com/products/media.aspx?type=brochure&id=279542>; Spies et al., 2001, 2004, 2007), Embosphere (CeloNova BioSciences, San Antonio, USA) (CeloNova BioSciences, 2014, <http://celonova.com/our-company/about-celonova/>; Stampfl et al., 2008, 2012) and LC beads (BTG International Ltd., London, UK) (BTG International Ltd., 2014, <http://www.btg-im.com/products/usa-323/lc-bead-70/about-lcbead>). In general, these microspheres with a size range of 40–1300 μm are introduced into the feeding artery of the tissue via fluoroscopy-guided catheterization, resulting in uniform artery occlusion with a predictable penetration depth (Chiesa and Hart, 2004;

* Corresponding author. Tel.: +31 88 75 509 34; fax: +31 88 75 558 50.

E-mail address: C.Oerlemans@umcutrecht.nl (C. Oerlemans).

Rasuli et al., 2008). Beside these 'bland' embolization particles, which neither possess image possibilities nor contain additional chemotherapeutic drugs, microspheres can be loaded with therapeutic compounds. The inclusion of chemotherapeutic drugs in embolization agents (e.g., microspheres) provides a locoregional drug delivery approach called transarterial (chemo) embolization (TACE/TAE). Currently, several drug-eluting beads (DEB) which contain doxorubicin (DEBDOX™) (Lewis and Holden, 2011) or irinotecan (DEBIRI™) (Lewis and Dreher, 2012) are commercially available for the treatment of liver cancer. A major drawback of the currently clinically available bland- and drug-loaded-microspheres, however, is that they cannot be visualized in vivo using medical imaging techniques, prohibiting any feedback on the microsphere distribution during and after the treatment. A microsphere formulation that can be visualized both by X-ray and MRI techniques, is expected to increase both the safety and the efficacy of embolotherapy procedures. More precisely, X-ray visibility offers the opportunity to real-time monitor the microsphere infusion using fluoroscopy, providing direct feedback for the interventional radiologist, which facilitates minimization of non-targeted delivery. However, if detailed knowledge of the microspheres with respect to the target and non-target tissue is required, MRI may be used as a complementary post-treatment technique, since MRI provides superior soft tissue contrast and may be highly sensitive to dedicated contrast agents (Seevinck et al., 2007). The goal of this study was to develop a multimodal imageable microsphere formulation for embolotherapy and to investigate its multimodality imaging properties in an in vitro and ex vivo model. To this purpose, alginate microspheres were prepared, incorporating lipiodol to provide X-ray visibility, and holmium, a paramagnetic element, which renders it an MRI-contrast agent.

2. Materials and methods

2.1. Materials

All chemicals and polymers were of commercial sources and were used as obtained. Sodium alginate (Protanal LF 240 D, Ph. Eur.) was a generous gift from FMC Biopolymer Ltd. (Girvan, Ayrshire, United Kingdom). Pluronic F-68 was obtained from Sigma-Aldrich (Steinheim, Germany). Holmium (III) chloride hexahydrate ($\text{HoCl}_3 \cdot 6\text{H}_2\text{O}$; 99.9%) was purchased from Metall rare earth Ltd. (Shenzhen, China). Lipiodol®, a radiopaque contrast

agent composed of iodinated ethyl esters of fatty acids from poppy seed oil with a total iodine content of 37% (w/w) (Lewis et al., 2012), which is frequently used for TAE/TACE procedures (Lewandowski et al., 2011), was purchased from Guerbet (Lipiodol Ultrafluide, Guerbet, Aulnay-Sous-Bois, France). Agarose multipurpose (MP) was obtained from Roche Applied Science (Mannheim, Germany). Manganese(II) chloride tetrahydrate ($\text{MnCl}_2 \cdot 4\text{H}_2\text{O}$; ACS reagent) and nitric acid (65%) were obtained from Merck (Darmstadt, Germany).

2.2. Alginate microsphere preparation

For the preparation of alginate microspheres, the JetCutter technique was used (Prusse et al., 2000), resulting in spherical particles with a predetermined size. Briefly, sodium alginate was dissolved in demineralized water under magnetic stirring at a concentration of 2% (w/v). Subsequently, lipiodol or poppy seed oil was added to the alginate solution under vigorous stirring to prepare a 1:1 alginate: oil (w/w) emulsion. 1% (w/v) Pluronic F-68 was added as a surfactant to stabilize the emulsion. Next, the alginate–oil emulsion was processed with the JetCutter which was equipped with a cutting tool consisting of 40 wires with a diameter of 100 μm . A nozzle diameter of 250 μm was used and the rotor speed was set to 4000 rpm. The droplets were allowed to solidify in solutions containing 25 mM of the chloride salt of holmium to form holmium–lipiodol–alginate microspheres (Ho–lip–ams) and holmium–poppy seed oil–alginate microspheres (Ho–pso–ams). The preparation of Ho–lip–ams is illustrated in Fig. 1. Non-ethiodized poppy seed oil was used as control. The alginate microspheres were allowed to cross-link for 2 h under gentle magnetic stirring. After three washing steps to remove excess cations, in which the microspheres were dispersed in surplus demineralized water, mildly vortexed and centrifuged to remove the excess water, the microspheres were collected and stored in demineralized water at room temperature.

2.3. Microsphere characterization and stability

Morphological examination and size distribution of Ho–pso–ams and Ho–lip–ams were investigated with light microscopy (magnification 4×10). To calculate the average size and its distribution, the diameters of 100 randomly selected microspheres were determined. For the determination of the total holmium content of the Ho–lip–ams, 500 mg of Ho–lip–ams was collected by

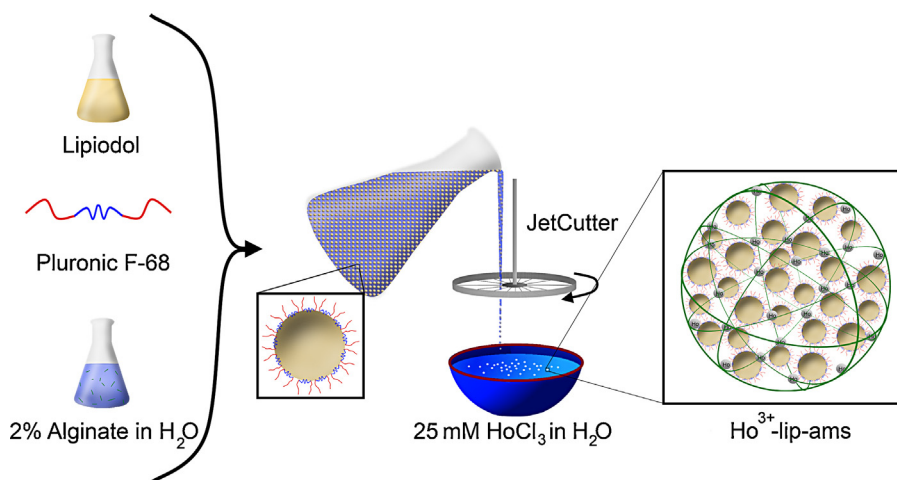


Fig. 1. Schematic drawing of Ho–lip–ams preparation. Lipiodol and water for injection are emulsified with Pluronic F-68. Next, the emulsion is processed with the JetCutter. The formed droplets fall into the holmium chloride solution resulting in the formation of holmium-cross-linked alginate microspheres entrapping lipiodol emulsified droplets (Ho–lip–ams).

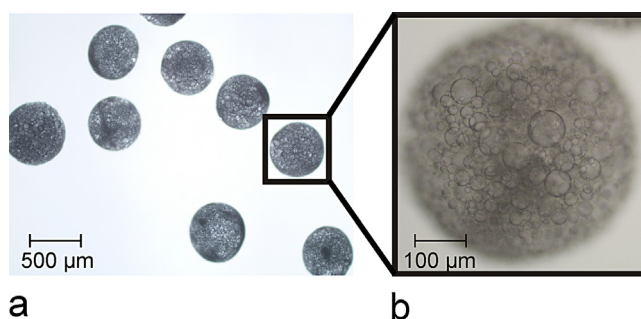


Fig. 2. Micrographs of Ho-lip-ams (magnification 4×10) (a), and $200 \times$ magnification of a single microsphere, which shows the lipidol emulsified droplets within the microspheres (b).

filtration using a $20 \mu\text{m}$ sieve to remove excess water. Next, the microspheres were destroyed in 10 mL of nitric acid (65%) at 100°C for 30 min. All samples were diluted in 2% nitric acid and measured on a Varian 820 MS (Varian, the Netherlands) with a detection limit of 0.1 ng mL^{-1} holmium using standard holmium reference material (Certipur Holmium ICP Standard, traceable to SRM from NIST, Merck, Darmstadt, Germany). To investigate the stability of Ho-lip-ams, microsphere samples (400 mg) were incubated in test tubes containing 10 mL fetal calf serum (FCS) and 5% penicillin/streptomycin to prevent bacterial and fungal growth. The test tubes were continuously shaken at 37°C for 14 consecutive days. After 4 h and every 24 h, the test tubes were centrifuged, and 1 mL of the supernatant was collected for microscopic examination and holmium content determination with inductively coupled plasma mass spectrometry (ICP-MS). The measurements were performed in duplicate.

2.4. In vitro phantoms containing alginate microspheres

For in vitro imaging of the Ho-pso-ams and Ho-lip-ams, a concentration series was prepared. The microspheres were embedded in agarose gel phantoms (1% w/w) containing 0.16 mM MnCl_2 to mimic the MRI relaxation properties of tissue as described previously (Seppenwoolde et al., 2005). The microsphere concentration in the sample tubes ranged from 0 to 196 mg mL^{-1} .

2.5. Intra-arterial Ho-lip-ams infusion in a porcine kidney

A porcine kidney from a small, 30 kg weighing female pig that was previously used as laboratory animal, was used to perform an ex vivo embolization procedure and mimic potential in vivo imaging applications. All experimental protocols and procedures applied on the pig prior to our ex vivo experiments were approved by the local experimental animal welfare committee and conform

national and European regulations for animal experimentation. The kidney was flushed with heparin solution to prevent coagulation of blood in the tissue and subsequently with demineralized water containing 0.16 mM MnCl_2 to reduce the longitudinal relaxation rate (T_1) of the water and to mimic the relaxation properties of tissue (Seppenwoolde et al., 2005). Next, the left renal vein and artery were ligated and the organ was extirpated. A catheter (Abbocath - T I.V. Catheter $20 \text{ g} \times 1.25''$, Hospira Inc., Lake Forest, IL, USA) was placed selectively in the inferior segmental renal artery and fixated with a suture. The kidney was placed in a plastic bucket and fixated to the sides of the bucket. A 30 cm flushing line connected to a three-way stopcock was connected to the catheter. Then, a 10 mL syringe was filled with 42 mg of Ho-lip-ams dispersed in water for and connected to the three-way stopcock for infusion. The microspheres were brought into suspension by cautiously shaking the syringe and administered through the catheter system into the kidney under subtraction fluoroscopy at 70 kV using a digital flat panel fluoroscopy system (Allura Xper FD, Philips Healthcare). After the procedure, the catheter was flushed with 50 mL solution of 0.16 mM MnCl_2 in demineralized water to ensure complete microsphere infusion.

2.6. Multimodality imaging

MR imaging of the microsphere phantoms was performed using a 3T clinical MR scanner (Philips Healthcare, Best, The Netherlands). The sample tubes were positioned parallel to the B_0 field in an 8-channel head coil. To assess the MR imaging properties of the microsphere formulations, a 3D multiple gradient echo sequence was used with the following imaging parameters: FOV of $96 \times 96 \times 8.5 \text{ mm}^3$, scan matrix of $192 \times 192 \times 17$, reconstruction matrix equal to scan matrix resulting in a reconstructed voxel size of 0.5 mm^3 , repetition time = 150 ms, echo time = 4.2 ms, echo spacing = 5 ms, 9 echoes, two signal averages and a 40° flip

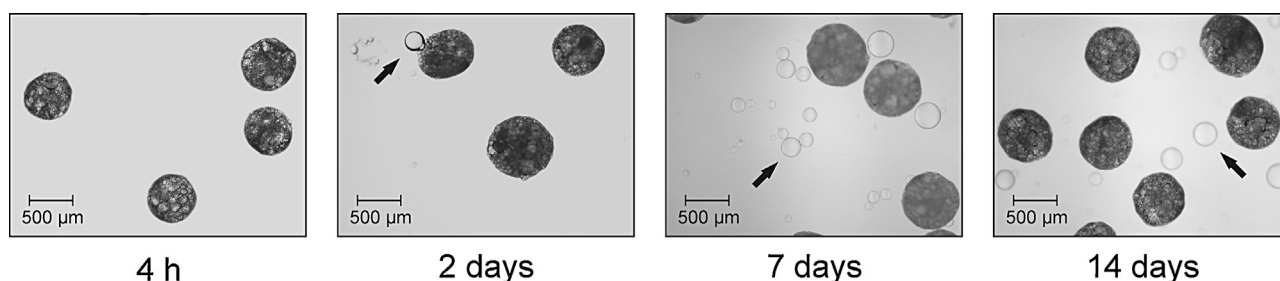


Fig. 3. Micrographs of Ho-lip-ams after 4 h, 2 days, 7 days and 14 days of incubation in fetal calf serum (magnification 4×10). The black arrows indicate small lipidol droplets.

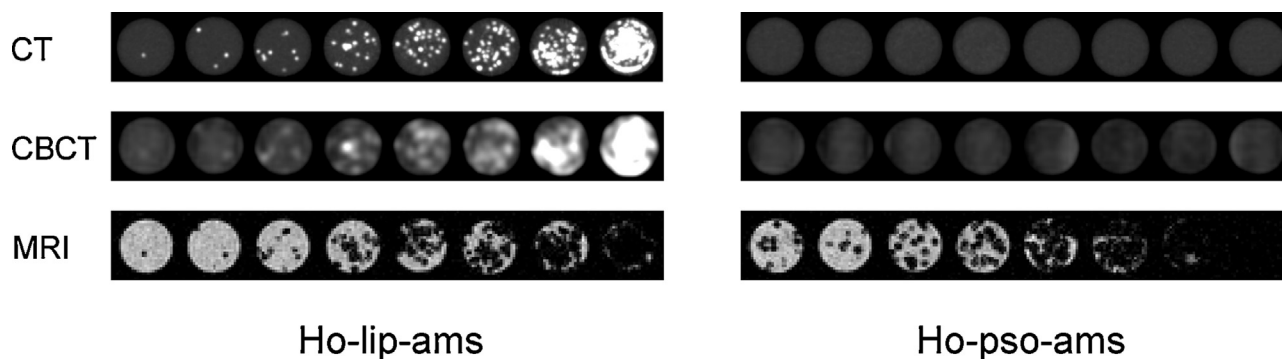


Fig. 4. Transverse images of a concentration series of Ho-lip-ams and Ho-pso-ams. The Ho-lip-ams can be depicted as single spheres using multimodality imaging (CT, CBCT and MRI). For Ho-pso-ams, only MRI allows for microsphere visualization due to the absence of radiopaque lipiodol. MR images are taken from the third echo (TE = 14.2 ms).

angle. After intra-arterial Ho-lip-ams infusion in a porcine kidney, MR imaging was performed using a 3D multiple gradient echo ultra short TE sequence with the following imaging parameters: FOV of $128 \times 128 \times 44 \text{ mm}^3$, scan matrix of $160 \times 160 \times 55$, reconstruction matrix of $256 \times 256 \times 55$ resulting in a reconstructed voxel size of $0.5 \times 0.5 \times 0.8 \text{ mm}^3$, repetition time = 17.2 ms, echo time = 0.14 ms, echo spacing = 1.4 ms, 5 echoes, two signal averages and a 15° flip angle. X-ray CT imaging of the sample tubes was performed on a clinical 64 slice CT scanner (Brilliance, Philips Medical Systems, Best, The Netherlands) at tube voltages of 80, 100, 120 and 140 kV using a soft tissue reconstruction filter. Imaging parameters included a FOV of $128 \times 128 \text{ mm}^2$, reconstruction matrix of 512×512 , slice thickness of 1.0 mm, increment of 0.5 mm, rotation time 0.5 s, collimation of $64 \times 0.625 \text{ mm}$, pitch of 0.673 and a tube current of 337 mA. For both Ho-pso-ams and Ho-lip-ams a linear regression curve was constructed to determine the sensitivity of X-ray CT (in HU mL mg^{-1}) for the alginate microsphere formulations using the methods as described by Seevinck et al. (2007). For high resolution CT imaging, allowing the visualization of the microspheres, the same parameters were used with the following modifications: slice thickness 0.67, increment of 0.33 mm, collimation of 20×0.625 and pitch of 0.656 measured at 120 kV. Furthermore, after intra-arterial infusion of Ho-lip-ams in the renal artery, an X-ray CT scan was made with the same imaging parameters as mentioned above with the following modifications: pitch of 0.652, FOV of $159 \times 159 \text{ mm}^2$ and a reconstruction matrix of 1024×1024 . Moreover, a cone beam rotational CT scan (CBCT) was obtained for the sample tubes and a porcine kidney after microsphere infusion using at standard abdominal scanning protocol (CT Abdomen fast HD protocol, XperCT, Philips Healthcare, Best, The Netherlands).

3. Results

3.1. Microsphere characterization and stability

A representative micrograph of Ho-lip-ams is shown in Fig. 2. The emulsified lipiodol is visible as small droplets of a size range around $10\text{--}80 \mu\text{m}$ dispersed in the alginate matrix. The holmium content of the Ho-lip-ams was $0.38 \pm 0.01\%$ (w/w). Inductively coupled plasma mass spectrometry (ICP-MS) measurements of fetal calf serum (FCS) in which Ho-lip-ams were incubated at 37°C for two weeks showed a holmium dissociation of $10.8 \pm 1.1\%$. This percentage was already reached after one day, while no further leakage was observed up to two weeks of exposure time, hence the holmium-alginate matrix of the Ho-lip-ams remained intact. Meanwhile, slow lipiodol release from the holmium-alginate matrix was observed over time (Fig. 3).

3.2. Multimodality imaging of alginate microspheres in vitro

CBCT, CT and MR imaging was performed on the alginate microsphere phantoms to demonstrate the possibility of individual microsphere detection on each modality. The spatial Ho-lip-ams distribution was comparable on each imaging technique, as is shown in Fig. 4. Ho-pso-ams were not detected with CBCT and CT imaging due to the absence of radiopaque iodine within the microspheres. Image stacks of the alginate microsphere phantoms showing the distribution of the Ho-lip-ams and Ho-pso-ams throughout the phantom concentration series can be found in the supplementary material (S1 and S2). Moreover, and in addition to

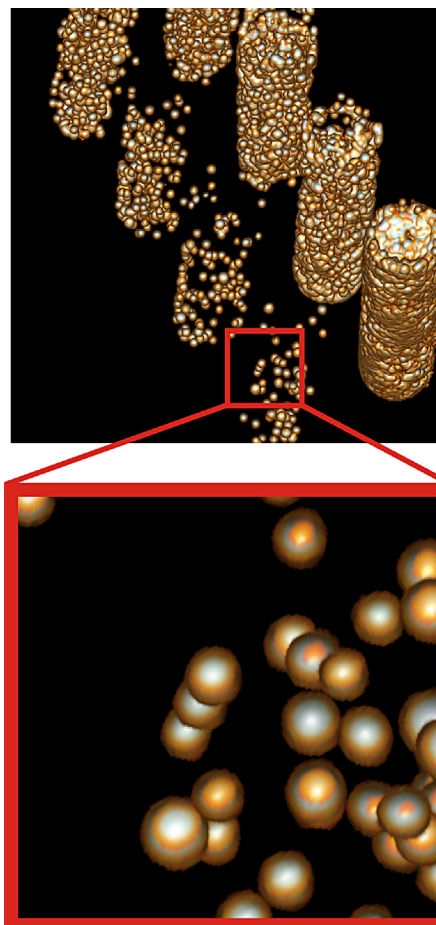


Fig. 5. Ho-lip-ams depicted as single spheres with 3-D CT assessment.

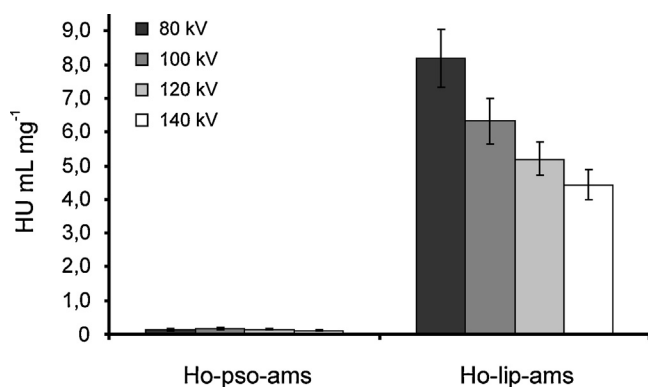


Fig. 6. CT sensitivity (in HU mL mg⁻¹) of Ho-pso-ams and Ho-lip-ams.

previous in-depth MR studies of alginate microspheres (Oerlemans et al., 2013), the sensitivity of CT for 3-D rendering of CT images illustrates the spatial distribution of the Ho-lip-ams as individual microspheres throughout the agarose phantoms (Fig. 5). The sensitivity of X-ray CT (in HU mL mg⁻¹) for the Ho-lip-ams and Ho-pso-ams is shown in Fig. 6. As expected, Ho-lip-ams had superior CT imaging properties as compared to Ho-pso-ams (a sensitivity increase ~60 times was observed at 80 kV). These results confirm the findings as shown in Fig. 4.

3.3. Ho-lip-ams infusion in a porcine kidney

In order to validate the possibilities for image-guided administration, the microspheres were administered under fluoroscopy-guidance via a catheter in a porcine kidney. Fig. 7 shows that the Ho-lip-ams were clearly visible under digital subtraction fluoroscopy during administration. A movie showing the fluoroscopy-guided infusion of the microspheres is available as supplementary material (S3). After the procedure, multimodality imaging was performed to determine the distribution of the microspheres in the kidney. Selective embolization of the inferior renal segment was achieved (Fig. 8). The fluoroscopy (Fig. 8a), CBCT (Fig. 8b), CT (Fig. 8c) and MR (Fig. 8d) images show a similar microsphere distribution and indicate that all four modalities are appropriate for Ho-lip-ams visualization, although with different

characteristics related to the intrinsic properties of the imaging modality. In the supplementary material (S4 and S5), additional image stacks are available showing the microsphere distribution throughout the tissue.

4. Discussion

Embolotherapy is a minimally invasive endovascular intervention technique and is currently regarded a standard treatment of a variety of (hypervascular) tumors. Nevertheless, the procedure as presently performed with commercially available microspheres does neither allow direct nor indirect visual feedback to the interventional radiologist, while imaging is crucial to increase the safety of the procedure and improve the outcome of the therapy for the patient. The possibility of intra-procedural imaging of the microsphere infusion would be beneficial for treatment optimization, while post-procedural assessment would allow visualization of the microspheres distribution throughout the tissue and provide predictive value for the outcome of the treatment. In this study, multimodality imageable microspheres, Ho-lip-ams, were successfully developed and detectable with high resolution on fluoroscopy, (CB)CT and MRI. The mean size (\pm SEM) of the Ho-lip-ams was $570 \pm 12 \mu\text{m}$, which is a clinically appropriate diameter for embolotherapy (Merit Medical, 2014, <http://www.merit.com/products/media.aspx?type=brochure&id=279542>). The size of the microspheres, however, is not limited to this range and can be tailored to fit a specific embolotherapy strategy by adjusting the settings of the JetCutter, enabling microsphere sizes between 120 and 3 mm (Genialab GmbH, 2014, <http://www.genialab.com/TechJetCutter.php>). The Ho-lip-ams showed good stability with only $10.8 \pm 1.1\%$ holmium dissociation after two weeks of incubation in fetal calf serum at 37 °C. Due to the relatively low holmium content within the Ho-lip-ams, toxicity of the microspheres is expected to be low. To illustrate, FDA-approved gadolinium-chelates, which are frequently used for MRI diagnostics, are administered in concentrations of 0.1 mmol kg^{-1} , from which 1% is dissociated (Wedeking et al., 1992). Holmium is a lanthanide comparable to gadolinium, and for a 100 kg patient receiving 1 g of microspheres (a regular amount for embolization), a total holmium concentration of 250 nmol kg^{-1} would be administered to the patient, which is 4 times lower as compared

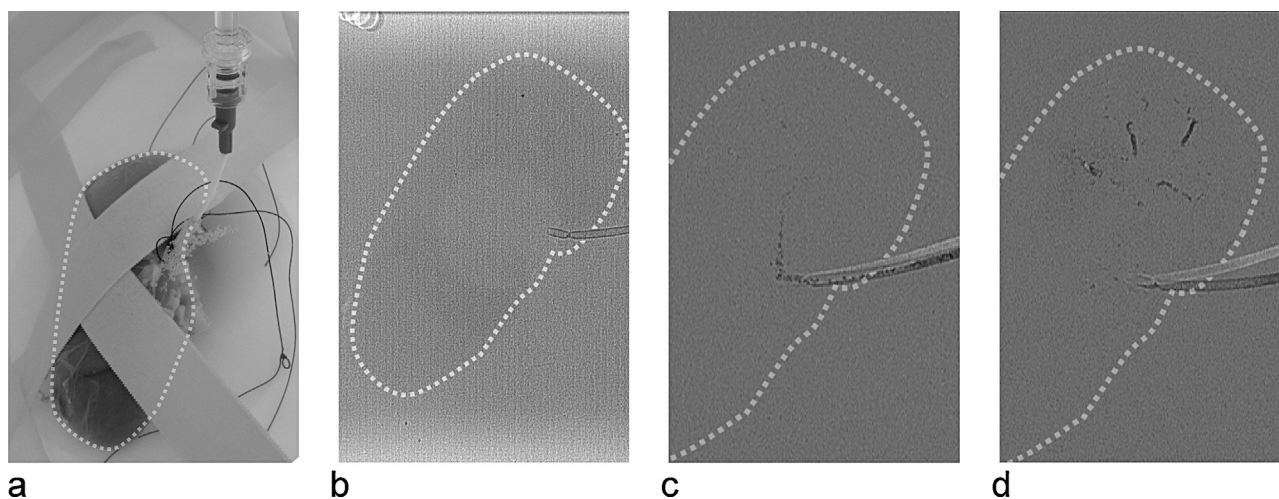


Fig. 7. Fluoroscopy-guided infusion of Ho-lip-ams in a porcine kidney. The kidney, which is delineated by the dotted line in this figure, was fixated to the inside of a plastic box and a catheter was inserted in the inferior segmental renal artery (a). Fluoroscopy of the kidney before microsphere infusion (b). Digital subtraction fluoroscopy of kidney during the embolization procedure (c, d).

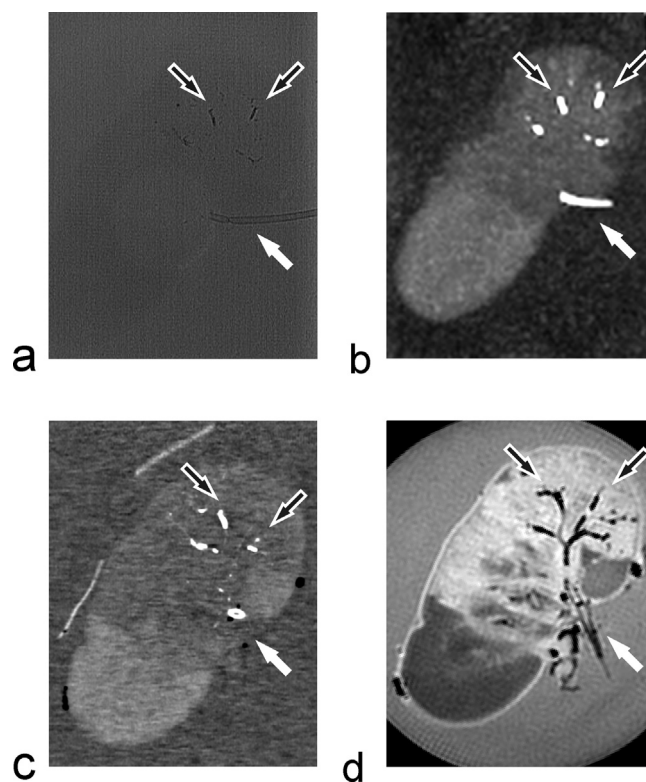


Fig. 8. Multimodal images of a porcine kidney after infusion of Ho-lip-ams. Fluoroscopy (a), CBCT (b), CT (c) and MRI (third echo, TE = 2.9 ms) (d). The black arrows indicate the clusters of microspheres deposited in the tissue. The white arrows show the catheter position on the different modalities.

to the 1% of dissociated gadolinium from gadolinium-chelates and even 40 times lower when taken into account the percentage of dissociated holmium from Ho-lip-ams. Moreover, slow lipiodol release from the microspheres was observed. This observation will be investigated in upcoming studies since it provides proof-of-concept as a slow-release drug delivery system, wherein lipiodol can be combined with a chemotherapeutic agent such as doxorubicin or cisplatin. The combination of lipiodol and drugs is currently frequently used in TACE procedures (Lo et al., 2002; Llovet et al., 2002), and its efficacy may be increased using the concept as presented in this study. In bland embolization, the procedure is continued until a desired embolization endpoint is reached or reflux of contrast material into non-target vessels is observed (Lewis et al., 2012). The novel microsphere formulation as presented here allows intra-procedural imaging of the embolization procedure as was demonstrated in a porcine kidney during an embolization procedure. This facilitates direct feedback of the microsphere administration and may therefore enable the possibility to modify the intervention and defining desirable embolization endpoints depending on observations made during the procedure (Sharma et al., 2010). Post-procedural imaging of the embolization procedure, which was shown with both (CB)CT and MRI, allows determination of microsphere distribution. This enables dosimetry (Seevinck et al., 2012), which would significantly improve the predictability of the treatment, especially when chemotherapeutic drugs are included in the microspheres. Another merit of the Ho-lip-ams is that its components are in compliance with the requirements of the European Pharmacopoeia, which would more easily facilitate the bench-to-bedside translation. The next steps include in vivo testing of the microspheres during an embolization procedure as well as post-procedural follow-up to investigate both systemic effects and the local effects of the microspheres on the targeted tissue.

5. Conclusion

In the present study, a new microsphere formulation for multimodality image-guided embolotherapy is presented. The combination of intra-procedural visualization, multimodality imaging for patient follow-up and the possibility of quantification offers a new and promising method for more safe, efficient and successful embolization treatment.

Appendix A. Supplementary data

Supplementary data associated with this article can be found, in the online version, at <http://dx.doi.org/10.1016/j.ijpharm.2014.11.010>.

References

- BTG International Ltd., 2014 <http://www.btg-im.com/products/usa-323/lc-bead-70/about-lcbead>(accessed 10.29.14.).
- CeloNova BioSciences, 2014 <http://celonova.com/our-company/about-celonova/> (accessed 10.29.14.).
- Chiesa, A.G., Hart, W.R., 2004. Uterine artery embolization of leiomyomas with trisacryl gelatin microspheres (TGM): pathologic features and comparison with polyvinyl alcohol emboli. *Int. J. Gynecol. Pathol.* 23, 386–392.
- Derdeyn, C.P., Moran, C.J., Cross, D.T., Dietrich, H.H., Dacey Jr., R.G., 1995. Polyvinyl alcohol particle size and suspension characteristics. *AJNR Am. J. Neuroradiol.* 16, 1335–1343.
- Genialab GmbH, 2014 <http://www.genialab.com/TechJetCutter.php>(accessed 10.29.14.).
- Lewandowski, R.J., Geschwind, J.F., Liapi, E., Salem, R., 2011. Transcatheter intraarterial therapies: rationale and overview. *Radiology* 259, 641–657.
- Lewis, A.L., Holden, R.R., 2011. DC Bead embolic drug-eluting bead: clinical application in the locoregional treatment of tumours. *Exp. Opin. Drug Deliv.* 8, 153–169.
- Lewis, A.L., Dreher, M.R., 2012. Locoregional drug delivery using image-guided intra-arterial drug eluting bead therapy. *J. Control. Release* 161, 338–350.
- Lewis, A.L., Holden, R.R., Chung, S.T., Czuczman, P., Kuchel, T., Finnie, J., et al., 2012. Feasibility, safety and pharmacokinetic study of hepatic administration of

- drug-eluting beads loaded with irinotecan (DEBIRI) followed by intravenous administration of irinotecan in a porcine model. *J. Mater. Sci. Mater. Med.* 24, 115–127.
- Lovet, J.M., Real, M.I., Montana, W., Planas, R., Coll, S., Aponte, J., et al., 2002. Arterial embolisation or chemoembolisation versus symptomatic treatment in patients with unresectable hepatocellular carcinoma: a randomised controlled trial. *Lancet* 359, 1734–1739.
- Lo, C.M., Ngan, H., Tso, W.K., Liu, C.L., Lam, C.M., Poon, R.T., et al., 2002. Randomized controlled trial of transarterial lipiodol chemoembolization for unresectable hepatocellular carcinoma. *Hepatology* 35, 1164–1171.
- Merit medical, 2014 <http://www.merit.com/products/media.aspx?type=brochure&id=279542>(accessed 10.29.14.).
- Oerlemans, C., Seevinck, P.R., van de Maat, G.H., Boulkhrif, H., Bakker, C.J., Hennink, W.E., Nijssen, J.F., 2013. Alginate-lanthanide microspheres for MRI-guided embolotherapy. *Acta Biomater.* 9, 4681–4687.
- Prusse, U., Dalluhn, J., Breford, J., Vorlop, K.D., 2000. Production of spherical beads by jetcutting. *Chem. Eng. Technol.* 23, 1105–1110.
- Rasuli, P., Hammond, I., Al-Mutairi, B., French, G.J., Aquino, J., Hadziomerovic, A., et al., 2008. Spherical versus conventional polyvinyl alcohol particles for uterine artery embolization. *J. Vasc. Interv. Radiol.* 19, 42–46.
- Seevinck, P.R., Seppenwoolde, J.H., de Wit, T.C., Nijssen, J.F., Beekman, F.J., van het Schip, A.D., et al., 2007. Factors affecting the sensitivity and detection limits of MRI, CT, and SPECT for multimodal diagnostic and therapeutic agents. *Anticancer Agents Med. Chem.* 7, 317–334.
- Seevinck, P.R., van de Maat, G.H., de Wit, T.C., Vente, M.A.D., Nijssen, J.F.W., Bakker, C.J.G., 2012. Magnetic resonance imaging-based radiation-absorbed dose estimation of 166-Ho microspheres in liver radioembolization. *Int. J. Rad. Oncol. Biol. Phys.* 83, e437–e444.
- Seppenwoolde, J.H., Nijssen, J.F., Bartels, L.W., Zielhuis, S.W., van het Schip, A.D., Bakker, C.J., 2005. Internal radiation therapy of liver tumors: qualitative and quantitative magnetic resonance imaging of the biodistribution of holmium-loaded microspheres in animal models. *Magn. Reson. Med.* 53, 76–84.
- Sharma, K.V., Dreher, M.R., Tang, Y., Pritchard, W., Chiesa, O.A., Karanian, J., Willis, S.L., Lewis, A.L., Wood, B.J., et al., 2010. Development of imageable beads for transcatheter embolotherapy. *J. Vasc. Interv. Radiol.* 21, 865–876.
- Spies, J.B., Benenati, J.F., Worthington-Kirsch, R.L., Pelage, J.P., 2001. Initial experience with use of tris-acryl gelatin microspheres for uterine artery embolization for leiomyomata. *J. Vasc. Interv. Radiol.* 12, 1059–1063.
- Spies, J.B., Allison, S., Flick, P., McCullough, M., Sterbis, K., Cramp, M., et al., 2004. Polyvinyl alcohol particles and tris-acryl gelatin microspheres for uterine artery embolization for leiomyomas: results of a randomized comparative study. *J. Vasc. Interv. Radiol.* 15, 793–800.
- Spies, J.B., Cornell, C., Worthington-Kirsch, R., Lipman, J.C., Benenati, J.F., 2007. Long-term outcome from uterine fibroid embolization with tris-acryl gelatin microspheres: results of a multicenter study. *J. Vasc. Interv. Radiol.* 18, 203–207.
- Stampfl, S., Stampfl, U., Bellemann, N., Sommer, C.M., Thierjung, H., Radeleff, B., et al., 2008. Biocompatibility and recanalization characteristics of hydrogel microspheres with polyzene-F as polymer coating. *Card. Interv. Radiol.* 31, 799–806.
- Stampfl, U., Sommer, C.M., Bellemann, N., Holzschuh, M., Kueller, A., et al. Kenngott, Bluemmel J., Kauczor, H.U., Radeleff, B., 2012. Multimodal visibility of a modified polyzene-F-coated spherical embolic agent for liver embolization: feasibility study in a porcine model. *J. Vasc. Interv. Radiol.* 23, 1225–1231.
- Wedeking, P., Kumar, K., Tweedle, M.F., 1992. Dissociation of gadolinium chelates in mice: relationship to chemical characteristics. *Magn. Reson. Imag.* 10, 641–648.